$1/f$ noise from the sequence of nonoverlapping rectangular pulses

Aleksejus Kononovicius [*] and Bronislovas Kaulakys [†]
Institute of Theoretical Physics and Astronomy, Vilnius University, Saulėtekio 3, Vilnius LT-10257, Lithuania

(Received 24 October 2022; revised 9 February 2023; accepted 24 February 2023; published 13 March 2023)

We analyze the power spectral density of a signal composed of nonoverlapping rectangular pulses. First, we derive a general formula for the power spectral density of a signal constructed from the sequence of nonoverlapping pulses. Then we perform a detailed analysis of the rectangular pulse case. We show that pure $1/f$ noise can be observed until extremely low frequencies when the characteristic pulse (or gap) duration is long in comparison to the characteristic gap (or pulse) duration, and gap (or pulse) durations are power-law distributed. The obtained results hold for the ergodic and weakly nonergodic processes.

DOI: 10.1103/PhysRevE.107.034117

I. INTRODUCTION

Flicker noise, also $1/f$ noise or pink noise, is a phenomenon well-known for almost a century since it was first observed by Johnson in a vacuum tube experiment [1,2]. Since then power-law scaling in the power spectral density of $1/f^{\beta}$ form (with $0.5 \lesssim \beta \lesssim 1.5$) has been reported in different experiments and empirical data sets across varied fields of research [3–7], especially in solids [8–10]. One of the peculiarities of $1/f$ noise is that it is observed for low frequencies and no cutoff frequency has been observed in many cases, e.g., 300 years' worth of weather data [11] or a three-week experiment with semiconductors [12], no cutoff frequency has been observed [13]. In other cases, the cutoff frequency can be observed [14–16], but $1/f$ noise is still observed over a broad range of frequencies.

Given observations in various research fields, one would expect that a general explanation of $1/f$ noise is due. However, even almost a century after discovery, there is no generally accepted model of $1/f$ noise. There are numerous different modeling approaches, some of them based on actual physical mechanisms within the systems in question, while some approaches aspire to provide a more general explanation. Mathematical literature is rich in true long-range memory models, such as fractional Brownian motion [17], ARCH family models [18], and ARFIMA models [19]. In physics literature, one most commonly will see $1/f$ noise being obtained by appropriately summing Lorentzian spectra as in the McWorther model [20,21]. Self-organized criticality framework was also put forward as a possible explanation [22], as well as the memoryless nonlinear response [23]. Our group has built various nonlinear stochastic processes to model $1/f$ noise in a variety of scenarios and different modeling frameworks: autoregressive interevent time point processes [21,24], stochastic differential equations [25,26], and agent-based models [27]. For a detailed review of works by our group see Ref. [28]. Our group, as well as others, have observed that nonlinear transformations of Markovian stochastic processes can lead to spurious long-range memory processes [29–32]. These are completely different approaches as the true long-range memory models rely on nonlocal operators, while the models exhibiting spurious long-range memory rely on locally nonlinear potentials, which often result in nonergodic or nonstationary behavior.

Here we will consider a different model, one which is not affected by the nonlinear transformations of amplitude and thus reproduces $1/f$ noise not due to fluctuations in amplitude but due to temporal dynamics. The approach we take here is most similar to renewal theory models [33] and random telegraph noise models, as we model a system which abruptly switches between two states ("on" and "off"). Thus the signal generated has the characteristic look of a telegraph signal or pulse sequence [34]. In Ref. [35], Halford suggested that $1/f$ noise could be modeled by a sequence of well-behaved perturbations with power-law distributed durations. Heiden [36] considered a sequence of pulses, with the coupling between pulse amplitude, duration, and the gap duration, and showed that for fixed-time integral pulses (of any arbitrary shape) $1/f^{\beta}$ noise will be obtained when the pulse duration is power-law distributed. In Ref. [37] an opposite problem was solved: reconstruction of pulse duration distribution given power spectral density and the characteristic pulse shape. Schick and Verveen have reported a grain flow experiment in which $1/f$ noise was observed with a low-frequency cutoff [14]. A theoretical model of triangular pulse sequences was also proposed to explain the experimental results. The power spectral density of a signal with "on" and "off" states was examined in [38]. The autocorrelation function of a random telegraph signal with power-law distributed "on" and "off" durations was obtained in Ref. [39]. Exploration of the nonergodic case has led to further exploration of age dependence of observed statistical properties [40] and a proposed solution to the cutoff paradox [13]. Theoretical and empirical analysis of $1/f$ noise in random telegraphlike signals remains an active object of research (for more recent examples see Refs. [41–47]). References [48,49] considered a combination of the random telegraphlike dynamics turning the Poisson process on and off as an explanation for $1/f$ noise in semiconductors. References [50–53] have considered the random

[*]aleksejus.kononovicius@tfai.vu.lt; https://kononovicius.lt.
[†]bronislovas.kaulakys@tfai.vu.lt

telegraphlike noise in the blinking quantum dots experiments, in some cases leading to the prediction and experimental observation of the aging effects in the power spectral densities. Therefore, this is a third kind of approach to the modeling of the long-range memory phenomenon, which is local in the event-time space, but is observed as nonlocal due to the observation occurring in the real-time space [26].

In this paper, we consider a sequence of nonoverlapping rectangular pulses and show that $1/f$ noise can be obtained when gap durations are short in comparison to the characteristic pulse duration and are power-law distributed. In Sec. II we provide a generalized derivation of an expression for the power spectral density of the signal constructed from the sequence of nonoverlapping pulses. In Sec. III we examine the case when the pulse and gap durations are sampled from the exponential distribution. In Sec. IV we examine a case when gap durations are sampled from a power-law distribution (bounded Pareto distribution is used for analytical derivations and numerical simulation), and examine the conditions when pure $1/f$ noise can be observed. We find that the range of frequencies over which $1/f$ noise is observed does nontrivially depend on the characteristic duration of the pulses. In Sec. V we explore the implications of finite observation time on the reported results, which yields a weakly nonergodic process exhibiting $1/f$ noise with low-frequency cutoff observable only for the extremely low frequencies. A summary of the obtained results is provided in Sec. VI.

II. POWER SPECTRAL DENSITY OF THE SEQUENCE OF NONOVERLAPPING PULSES

We investigate a stochastic process generating a sequence of nonoverlapping pulses with random durations θ_k. The pulses are separated by gaps of random duration τ_k. In the general case this stochastic process generates a signal which is given by a sum over all pulse profiles $A_k(t)$ when the respective pulse occurs at time t_k:

$$I(t) = \sum_k A_k(t - t_k). \tag{1}$$

Note that we assume that $A_k(s)$ may have nonzero values only during the pulse. Before the pulse starts ($s < 0$) and after the pulse ends ($s > \theta_k$), $A_k(s)$ is assumed to be zero. The truncation of pulse profiles and the gaps between the pulses ensure that the pulses never overlap or touch. As the pulses are nonoverlapping, t_k is given by a sum of previous pulse and gap durations:

$$t_k = \sum_{q=0}^{k-1}(\theta_q + \tau_q). \tag{2}$$

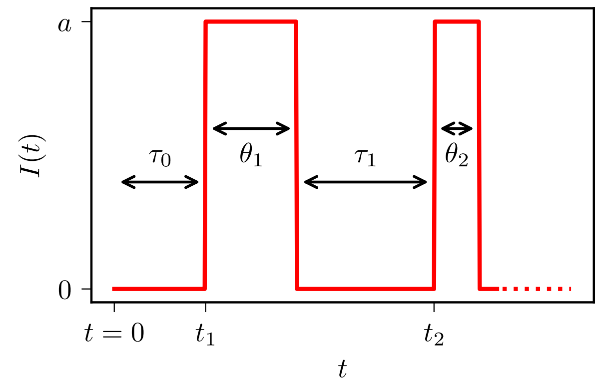

FIG. 1. Sample signal constructed from the sequence of nonoverlapping pulses (red curve): τ_q respective gap durations, θ_q respective pulse durations, t_k respective pulse occurrence time, a height of the rectangular pulses.

Here, for notational simplicity, we have chosen that $\theta_0 = 0$. When calculating the power spectral density of the signal we ignore this artificially introduced "zeroth" pulse. In Fig. 1 we have plotted a sample signal constructed from the sequence of nonoverlapping pulses and highlighted the aforementioned quantities. Note that if we allow pulses to be almost instantaneous (if we take $\theta_q \to 0$ limit), then we obtain a point process case.

The power spectral density of the signal $I(t)$ is given by

$$S(f) = \lim_{T\to\infty}\left\langle \frac{2}{T}\left|\int_0^T I(t)e^{-2\pi i f t}\mathrm{d}t\right|^2\right\rangle = \lim_{T\to\infty}\left\langle \frac{2}{T}\left|\sum_k e^{-2\pi i f t_k}F_k(f)\right|^2\right\rangle, \tag{3}$$

where the averaging $\langle\ldots\rangle$ is performed over distinct realizations of the process, T is the duration of the signal, and $F_k(f)$ is the Fourier transform of the kth pulse profile. For rectangular pulses, the Fourier transform is given by

$$F_k(f) = \int_0^{\theta_k} A_k(u)e^{-2\pi i f u}\mathrm{d}u = a\int_0^{\theta_k} e^{-2\pi i f}\mathrm{d}u = \frac{ia}{2\pi f}\left(e^{-2\pi i f\theta_k} - 1\right), \tag{4}$$

but at this point, let us keep our derivation general until the rectangular shape of the pulses is relevant. Let us split the expression for the power spectral density into two terms:

$$\begin{aligned} S(f) &= \lim_{T\to\infty}\left\langle \frac{2}{T}\sum_k\sum_{k'} e^{2\pi i f(t_{k'}-t_k)}F_k(f)F_{k'}^*(f)\right\rangle \\ &= \lim_{T\to\infty}\left\langle \frac{2}{T}\sum_k |F_k(f)|^2\right\rangle + \lim_{T\to\infty}\left\langle \frac{2}{T}\left(\sum_k\sum_{k'>k} e^{2\pi i f(t_{k'}-t_k)}F_k(f)F_{k'}^*(f) + \sum_k\sum_{k'<k} e^{2\pi i f(t_{k'}-t_k)}F_k(f)F_{k'}^*(f)\right)\right\rangle \\ &= S_1(f) + S_2(f), \end{aligned} \tag{5}$$

so we can deal with them separately. The first term trivially simplifies to

$$S_1(f) = 2\bar{\nu}\langle|F_k(f)|^2\rangle, \quad (6)$$

where $\bar{\nu}$ is the mean number of pulses per unit time. If the process is ergodic, and the observation time is long, then the mean value of $\bar{\nu}$ can be trivially obtained from the mean values of the pulse and gap durations, i.e., $\bar{\nu} = \frac{1}{\langle\theta\rangle+\langle\tau\rangle}$. For nonergodic processes, or if the observation time is short, then $\bar{\nu}$ needs to be defined as an empirical mean number, i.e., $\bar{\nu} = K/T$ (here K is the number of observed pulses). The two sums in the second term differ only in the sign of their imaginary parts, thus the second term can be rearranged by considering only the real part:

$$S_2(f) = 4\mathrm{Re}\left[\lim_{T\to\infty}\left\langle\frac{1}{T}\sum_{k}\sum_{k'>k} e^{2\pi \mathrm{i} f(t_{k'}-t_k)}F_k(f)F_{k'}^*(f)\right\rangle\right]. \quad (7)$$

The time difference $t_{k'} - t_k$ is the sum of the pulse and gap durations in between the k'th and kth pulses:

$$t_{k'} - t_k = \sum_{q=k}^{k'-1}(\theta_q + \tau_q). \quad (8)$$

Let the durations θ_q and τ_q be independently sampled from the arbitrarily selected distributions of pulse and gap durations, then the second term of the power spectral density can be rearranged as

$$S_2(f) = 4\bar{\nu}\mathrm{Re}\left[\langle e^{2\pi \mathrm{i} f\theta_k}F_k(f)\rangle\langle F_{k'}^*(f)\rangle\chi_\tau(f) \times \sum_{q=1}^{\infty}\chi_\theta(f)^{q-1}\chi_\tau(f)^{q-1}\right]. \quad (9)$$

In the above, we have introduced the characteristic functions of pulse $\chi_\theta(f) = \langle e^{2\pi \mathrm{i} f\theta_k}\rangle$ and gap $\chi_\tau(f) = \langle e^{2\pi \mathrm{i} f\tau_k}\rangle$ duration distributions. Here we have effectively replaced averaging over distinct realizations by averaging over the distribution of either pulse or gap durations.

Evaluating the summation over q simplifies the second term further:

$$S_2(f) = 4\bar{\nu}\mathrm{Re}\left[\langle e^{2\pi \mathrm{i} f\theta_k}F_k(f)\rangle\langle F_{k'}^*(f)\rangle\frac{\chi_\tau(f)}{1-\chi_\theta(f)\chi_\tau(f)}\right]. \quad (10)$$

Thus, the general expression for the power spectral density is

$$S(f) = 2\bar{\nu}\langle|F_k(f)|^2\rangle + 4\bar{\nu}\mathrm{Re}\left[\langle e^{2\pi \mathrm{i} f\theta_k}F_k(f)\rangle\langle F_{k'}^*(f)\rangle\frac{\chi_\tau(f)}{1-\chi_\theta(f)\chi_\tau(f)}\right]. \quad (11)$$

Let us now use the assumption that the pulses have rectangular shape, inserting Eq. (4) into Eq. (11) yields

$$S(f) = \frac{a^2\bar{\nu}}{\pi^2 f^2}\mathrm{Re}\left[\frac{(1-\chi_\theta(f))(1-\chi_\tau(f))}{1-\chi_\theta(f)\chi_\tau(f)}\right]. \quad (12)$$

Note that the above general expression for the power spectral density of a signal constructed from the rectangular nonoverlapping pulses implies that pulse and gap duration distributions are interchangeable. We will break this symmetry in a later section of the paper by making specific assumptions about pulse and gap duration distributions. Our conclusions will be formulated in accordance with the assumptions, but if the assumptions would be swapped (i.e., assumptions about pulse duration distribution would be made about gap duration distribution and vice versa), so the conclusions could be swapped, but otherwise would remain unchanged due to the symmetric nature of Eq. (12).

From Eq. (11) we can obtain the power spectral density of the shot noise. This can be achieved by taking the Poisson point process limit, i.e., assuming infinitesimal constant pulse durations θ, a constant pulse area $B = a\theta$, and independent exponentially distributed τ,

$$S_{\mathrm{shot}}(f) = 2B^2\bar{\nu}. \quad (13)$$

As should be expected, the expression above is identical to the well-known Schottky's formula [54] with $\langle I\rangle = B\bar{\nu}$.

For the low frequencies $f \ll (2\pi\langle\theta\rangle)^{-1}$ and $f \ll (2\pi\langle\tau\rangle)^{-1}$, when the distributions of the pulse and gap durations have finite variance $\sigma_\theta^2 = \langle\theta^2\rangle - \langle\theta\rangle^2 < \infty$ and $\sigma_\tau^2 = \langle\tau^2\rangle - \langle\tau\rangle^2 < \infty$, the characteristic functions can be expanded in the power series

$$\chi_\theta(f) = \langle e^{2\pi \mathrm{i} f\theta}\rangle \approx 1 + 2\pi \mathrm{i} f\langle\theta\rangle - 2\pi^2 f^2\langle\theta^2\rangle,$$
$$\chi_\tau(f) = \langle e^{2\pi \mathrm{i} f\tau}\rangle \approx 1 + 2\pi \mathrm{i} f\langle\tau\rangle - 2\pi^2 f^2\langle\tau^2\rangle. \quad (14)$$

Then from Eq. (12) it follows that the white noise will be observed for the low frequencies

$$S(f) \approx 2a^2\bar{\nu}\frac{\langle\theta\rangle^2\sigma_\tau^2 + \langle\tau\rangle^2\sigma_\theta^2}{(\langle\theta\rangle + \langle\tau\rangle)^2}. \quad (15)$$

On the other side of the frequency spectrum, when $\chi_\theta(f) \to 0$ and $\chi_\tau(f) \to 0$, from Eq. (12) Brownian-like noise is obtained:

$$S(f) \approx \frac{a^2\bar{\nu}}{\pi^2}\times\frac{1}{f^2}. \quad (16)$$

For the intermediate frequencies the power spectral density will depend on the explicit choice of pulse and gap duration distributions. In the following sections we investigate the possibility to observe $1/f$ noise, i.e., the signal with the power spectrum $S(f) \sim f^{-\beta}$ with $\beta \simeq 1$, in an arbitrarily broad range of intermediate frequencies.

III. EXPONENTIALLY DISTRIBUTED PULSE AND GAP DURATIONS

Let us first consider pulse durations sampled from the exponential distribution

$$p(\theta) = \frac{1}{\theta_c}\exp\left(-\frac{\theta}{\theta_c}\right). \quad (17)$$

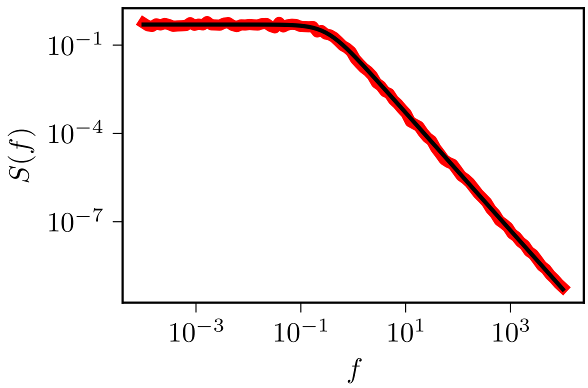

FIG. 2. Power spectral density of the signal when pulse and gap durations are sampled from exponential distribution. Red curve corresponds to a numerical simulation conducted with $a = 1$ and $\theta_c = \tau_c = 1$ (or, alternatively, $\gamma_\theta = \gamma_\tau = 1$). Black curve corresponds to Eq. (20).

In the above, we have introduced a notation for the mean duration of a pulse $\theta_c = \langle \theta \rangle$. The characteristic function of the exponential pulse duration distribution is

$$\chi_\theta(f) = \frac{1}{1 - 2\pi \mathrm{i} \theta_c f}. \tag{18}$$

The exponential distribution is our first choice as it is commonly observed in physical systems (e.g., the lifetime of conductive electrons in semiconductors is known to be exponentially distributed [55], chemical reactions are often modeled assuming exponential interevent times [56]), and socioeconomic systems (e.g., times between goals scored by a football team seems to follow exponential distribution [57], infection times in the classical SIR model and adoption times in the Bass diffusion model also follow exponential distribution [58]).

Inserting Eq. (18) into Eq. (12) yields

$$S(f) = 4a^2 \bar{\nu} \theta_c^2 \mathrm{Re}\left[\frac{1}{1 - \chi_\tau(f) - 2\pi \mathrm{i} f \theta_c}\right]. \tag{19}$$

If gap durations are also sampled from the exponential distribution, but with mean τ_c, then from Eq. (19) it follows that Brownian-like noise will be observed:

$$S(f) = \frac{4a^2 \bar{\nu}}{(\gamma_\theta + \gamma_\tau)^2 + 4\pi^2 f^2}. \tag{20}$$

In the above $\gamma_\theta = \theta_c^{-1}$ and $\gamma_\tau = \tau_c^{-1}$ are the corresponding relaxation rates (inverses of the mean durations). As can be seen in Fig. 2, Eq. (20) agrees with numerically simulated power spectral density rather well.

IV. POWER-LAW DISTRIBUTED GAP DURATIONS

Power-law distributions are observed universally across a variety of empirical datasets from both natural and social sciences [59–62]. Some of the experiments, such as quantum dot fluorescence [50,63], single-particle tracking in biological systems [64], and animal movement observations [65], also exhibit signals with nonoverlapping pulses, signatures of anomalous diffusion, and long-range memory. There are also earlier theoretical works which suggest that $1/f^\beta$ noise will be observed when pulse or gap durations are sampled from power-law distributions [13,35,36,39,40]. While some of the aforementioned works focus on modeling of particular systems, there are no obvious limitations to interpret the reported results more broadly. Therefore let us investigate how the power spectral density of the signal with nonoverlapping rectangular pulses changes when the gap durations are sampled not from the exponential distribution, but from the power-law distribution. In contrast to earlier works in this section we will show that point processes (with instantaneous pulses) cannot yield pure $1/f$ noise, while a processes generating nonoverlapping rectangular pulses under certain conditions will yield pure $1/f$ noise.

Let us consider gap durations being sampled from the bounded Pareto distribution

$$p(\tau) = \begin{cases} \frac{\alpha \tau_{\min}^\alpha}{1 - \left(\frac{\tau_{\min}}{\tau_{\max}}\right)^\alpha} \times \frac{1}{\tau^{\alpha+1}} & \text{for } \tau_{\min} \leqslant \tau \leqslant \tau_{\max}, \\ 0 & \text{otherwise,} \end{cases} \tag{21}$$

with $\alpha > 0$. Instead of sharp cutoffs, one could consider smooth, e.g., exponential cutoffs. Smooth cutoffs would not significantly impact the expressions we derive further, but here we derive expressions for the sharp cutoffs as they are easier to deal with analytically and numerically. Also note that we could have alternatively assumed that pulse durations are being sampled from the bounded Pareto distribution instead. The choice which durations are sampled from the bounded Pareto distribution does not matter as the general expression for the power spectral density [Eq. (12)] is symmetric in respect to the characteristic functions.

The characteristic function of the bounded Pareto gap duration distribution is given by

$$\chi_\tau(f) = \frac{\alpha(-2\pi \mathrm{i} f \tau_{\min}\tau_{\max})^\alpha}{\tau_{\max}^\alpha - \tau_{\min}^\alpha}[\Gamma(-\alpha, -2\pi \mathrm{i} f \tau_{\min}) - \Gamma(-\alpha, -2\pi \mathrm{i} f \tau_{\max})]. \tag{22}$$

In the above, $\Gamma(s, x)$ is the upper incomplete Gamma function, defined as $\Gamma(s, x) = \int_x^\infty t^{s-1} e^{-t} dt$.

For $0 < \alpha < 2$, with notable exception of $\alpha = 1$, and $\frac{1}{2\pi\tau_{\max}} \ll f \ll \frac{1}{2\pi\tau_{\min}}$ the characteristic function can be approximated as

$$\chi_\tau(f) = \frac{\alpha(-2\pi \mathrm{i} f \tau_{\min}\tau_{\max})^\alpha}{\tau_{\max}^\alpha - \tau_{\min}^\alpha}\Gamma(-\alpha, -2\pi \mathrm{i} f \tau_{\min}) \approx 1 + \frac{\alpha}{\alpha - 1} \times (2\pi \mathrm{i} f \tau_{\min}) - \Gamma(1-\alpha) \times (-2\pi \mathrm{i} f \tau_{\min})^\alpha. \tag{23}$$

Inserting this approximation of the gap duration distribution characteristic function into Eq. (19) yields

$$S(f) = 4a^2\bar{\nu}\theta_c^2 \mathrm{Re}\left[\frac{1}{1-\frac{\alpha}{\alpha-1}\times(2\pi\mathrm{i}f\tau_{\min})+\Gamma(1-\alpha)\times(-2\pi\mathrm{i}f\tau_{\min})^{\alpha}-2\pi\mathrm{i}f\theta_c}\right]$$
$$\approx \frac{4a^2\bar{\nu}\theta_c^2(2\pi f\tau_{\min})^{\alpha}\cos\left(\frac{\pi\alpha}{2}\right)\Gamma(1-\alpha)}{\frac{4\pi^2f^2}{(\alpha-1)^2}[(\alpha-1)\theta_c+\alpha\tau_{\min}]^2+(2\pi f\tau_{\min})^{2\alpha}\Gamma(1-\alpha)^2}. \quad (24)$$

Assuming that the pulse durations are short ($\theta_c \ll \tau_{\min}$), two distinct cases are obtained: for $0 < \alpha < 1$ the power spectral density can be approximated by

$$S(f) = 4a^2\bar{\nu}\theta_c^2 \frac{\cos\left(\frac{\pi\alpha}{2}\right)}{(2\pi\tau_{\min})^{\alpha}\Gamma(1-\alpha)} \times \frac{1}{f^{\alpha}}, \quad (25)$$

while for $1 < \alpha < 2$ the power spectral density can be approximated by

$$S(f) = 4a^2\bar{\nu}\theta_c^2 \frac{(\alpha-1)^2\cos\left(\frac{\pi\alpha}{2}\right)\Gamma(1-\alpha)}{\alpha^2(2\pi\tau_{\min})^{2-\alpha}} \times \frac{1}{f^{2-\alpha}}. \quad (26)$$

The peculiar dependence of the power-law slope of the power spectral density is a result of different terms in the numerator of Eq. (24) becoming important for the low frequencies: for $0 < \alpha < 1$ the $f^{2\alpha}$ term is the most significant, while for $1 < \alpha < 2$ the f^2 term dominates.

If pulse durations are long in comparison to gap durations ($\theta_c \gg \tau_{\min}$), then f^2 term dominates, and thus the power spectral density can be approximated by

$$S(f) = 4a^2\bar{\nu}\frac{\tau_{\min}^{\alpha}\Gamma(1-\alpha)\cos\left(\frac{\pi\alpha}{2}\right)}{(2\pi)^{2-\alpha}} \times \frac{1}{f^{2-\alpha}}. \quad (27)$$

The approximations above suggest that in $\alpha = 1$ case $1/f$ noise should be observed, but the approximations diverge (and thus do not apply) in that case. The obtained approximations are qualitatively consistent with Refs. [35,36], though the distinction between comparatively short $\theta_c \ll \tau_{\min}$ and comparatively long $\theta_c \gg \tau_{\min}$ pulses was not made in the earlier papers.

With $\alpha = 1$ and for $\frac{1}{2\pi\tau_{\max}} \ll f \ll \frac{1}{2\pi\tau_{\min}}$ the characteristic function of the gap duration distribution can be instead approximated by

$$\chi_{\tau}(f) = 1 - \pi^2 f\tau_{\min} + [1 - C_{\gamma} - \ln(2\pi f\tau_{\min})] \times (2\pi\mathrm{i}f\tau_{\min}). \quad (28)$$

In the above, $C_{\gamma} = 0.577\ldots$ is the Euler's gamma constant. Inserting Eq. (28) into Eq. (19) yields

$$S(f) = \frac{a^2\bar{\nu}\tau_{\min}}{\left(\frac{\pi\tau_{\min}}{2\theta_c}\right)^2 + \left\{1 + \frac{\tau_{\min}}{\theta_c}[1 - C_{\gamma} - \ln(2\pi\tau_{\min}f)]\right\}^2} \times \frac{1}{f}. \quad (29)$$

Then for the short pulses $\theta_c \ll \tau_{\min}$, $\ln(f)$ term is non-negligible and thus the $1/f$ dependence will be perverted by an additional term dependent logarithmically on f:

$$S(f) = \frac{a^2\bar{\nu}\theta_c^2}{\tau_{\min}\left\{\left(\frac{\pi}{2}\right)^2 + [1 - C_{\gamma} - \ln(2\pi\tau_{\min}f)]^2\right\}} \times \frac{1}{f}. \quad (30)$$

While assumption that the pulse durations are long in comparison to the gap durations, $\theta_c \gg \tau_{\min}$ yields pure $1/f$ noise:

$$S(f) = a^2\bar{\nu}\tau_{\min} \times \frac{1}{f}. \quad (31)$$

For the comparatively long pulses $\theta_c \gg \tau_{\min}$, most reasonable parameter sets and ranges of frequencies $\ln(f)$ term will be negligible. The logarithmic term is non-negligible only for extremely low frequencies:

$$f \lesssim f^{(c)} = \frac{1}{2\pi\tau_{\min}} \exp\left[-(\sqrt{2}-1)\frac{\theta_c}{\tau_{\min}}\right]. \quad (32)$$

As shown in Fig. 3, the logarithmic term has significant impact in distorting $1/f$ dependence when pulses are short, while for the comparatively long pulses pure $1/f$ noise is observed. Influence of the logarithmic term is not observed in our simulation with the comparatively long pulses, because for the selected parameter values $f^{(c)} \approx 10^{-180}$, which is well outside the reasonably observable range of frequencies.

As long as pulse durations aren't short, pure $1/f$ noise should be observed with any other pulse duration distribution, as for $f \ll \frac{1}{2\pi\tau_{\min}}$ the characteristic function of the pulse duration distribution cancels out from Eq. (12). Thus from Eqs. (12) and (28) we have that

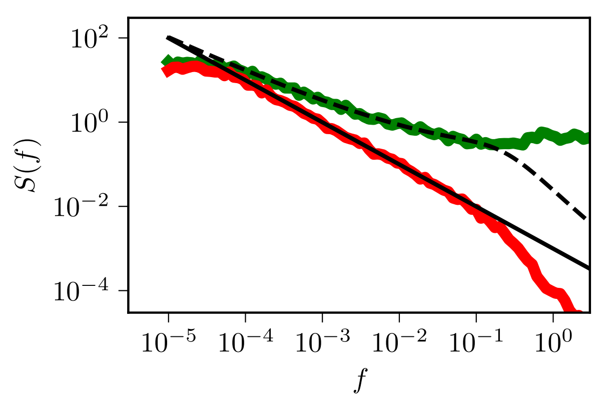

FIG. 3. Comparison of the power spectral densities in the $\alpha = 1$ case. Red curve shows the case with the comparatively long exponential pulse durations (simulated with $a = 1$, $\theta_c = 10^3$), while green curve shows the case with the comparatively short exponential pulse durations (simulated with $a = 10^3$, $\theta_c = 10^{-3}$). Black curves correspond to Eqs. (31) (solid) and (30) (dashed). Other simulation parameters: $\tau_{\min} = 1$ and $\tau_{\max} = 10^4$.

$$\begin{aligned} S(f) &= \frac{a^2\bar{\nu}}{\pi^2 f^2}\mathrm{Re}\left[\frac{(1-\chi_\theta(f))\times(\pi^2 f\tau_{\min}-[1-C_\gamma-\ln(2\pi f\tau_{\min})]\times(2\pi \mathrm{i} f\tau_{\min}))}{1-\chi_\theta(f)\times(1-\pi^2 f\tau_{\min}+[1-C_\gamma-\ln(2\pi f\tau_{\min})]\times(2\pi \mathrm{i} f\tau_{\min}))}\right] \\ &\approx \frac{a^2\bar{\nu}}{\pi^2 f^2}\mathrm{Re}\left[\frac{(1-\chi_\theta(f))\times(\pi^2 f\tau_{\min}-[1-C_\gamma-\ln(2\pi f\tau_{\min})]\times(2\pi \mathrm{i} f\tau_{\min}))}{1-\chi_\theta(f)}\right] \\ &= a^2\bar{\nu}\tau_{\min}\times\frac{1}{f}. \end{aligned} \tag{33}$$

This result matches what we have obtained for exponentially distributed pulse durations [Eq. (31)] and is further confirmed by the numerical simulations shown in Fig. 4. Indeed, this general result should hold well for the different possible selections of pulse duration distributions for an arbitrarily broad range of frequencies with extremely low cutoff frequency, $\max(\frac{1}{2\pi\tau_{\max}}, \frac{1}{2\pi\tau_{\min}}\exp[-(\sqrt{2}-1)\frac{\theta_c}{\tau_{\min}}]) \ll f \ll \frac{1}{2\pi\tau_{\min}}$.

V. AGING EFFECTS IN WEAKLY NONERGODIC CASE

As the approximation of the power spectral density [Eq. (31)] doesn't explicitly depend on the maximum bound of the gap duration distribution $\tau_{\max}$, gap durations could also be sampled from the Pareto distribution without an upper bound. Sampling from the Pareto distribution would yield a weakly nonergodic process similar to the one analyzed in Ref. [13]. The issue is that the approximation Eq. (31) does implicitly depend on $\tau_{\max}$ via $\bar{\nu}$. Thus, sampling from the Pareto distribution should introduce aging effects (i.e., integral of power spectral density will depend on the observation time T). In this section, we first derive an approximation for $\bar{\nu}$ in the ergodic case, and then we consider the weakly nonergodic case when the gap durations are sampled from the Pareto distribution.

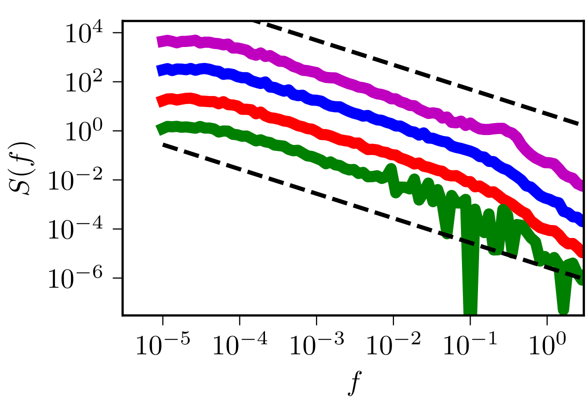

FIG. 4. Power spectral densities of a signal with rectangular pulses obtained sampling pulse durations from various distributions: exponential (red curve), degenerate (green), uniform (blue), and bounded Pareto (magenta) distributions. Gap durations were sampled from bounded Pareto distribution with $\alpha = 1$, $\tau_{\min} = 1$ and $\tau_{\max} = 10^4$. Dashed black lines have $1/f$ slope. Other simulation parameters: $a = 1$ and $\theta_c = 10^3$ (with exponential distribution), $a = 10^{-1}$ and $\theta_c = 10^2$ (degenerate distribution), $a = 3$, $\theta_{\min} = 0$ and $\theta_{\max} = 10^3$ (uniform distribution), $a = 3$, $\alpha_\theta = 1$, $\theta_{\min} = 1$, and $\theta_{\max} = 10^4$ (bounded Pareto distribution).

The mean of the bounded Pareto gap duration distribution is given by

$$\langle\tau\rangle = \begin{cases} \frac{\tau_{\max}\tau_{\min}}{\tau_{\max}-\tau_{\min}}\ln\left(\frac{\tau_{\max}}{\tau_{\min}}\right) & \text{for } \alpha = 1, \\ \frac{\alpha}{\alpha-1}\times\frac{\tau_{\max}^\alpha\tau_{\min}^\alpha}{\tau_{\max}^\alpha-\tau_{\min}^\alpha}\times\left(\frac{1}{\tau_{\min}^{\alpha-1}}-\frac{1}{\tau_{\max}^{\alpha-1}}\right) & \text{otherwise.} \end{cases} \tag{34}$$

For $\tau_{\max} \gg \tau_{\min}$ it can be approximated as:

$$\langle\tau\rangle \approx \begin{cases} \tau_{\min}\ln\left(\frac{\tau_{\max}}{\tau_{\min}}\right) & \text{for } \alpha = 1, \\ \frac{\alpha}{1-\alpha}\tau_{\max}\left(\frac{\tau_{\min}}{\tau_{\max}}\right)^\alpha & \text{for } 0 < \alpha < 1, \\ \frac{\alpha}{\alpha-1}\tau_{\min} & \text{for } \alpha > 1. \end{cases} \tag{35}$$

Note that for $\alpha > 1$ case the approximation of the mean is independent of $\tau_{\max}$ and matches the mean of the Pareto distribution without the upper bound.

If we assume that pulse duration is sampled from the exponential distribution or another narrow distribution, then we can approximate the mean number of pulses per unit time as

$$\bar{\nu} = \frac{1}{\langle\theta\rangle + \langle\tau\rangle} \approx \begin{cases} \frac{1}{\theta_c+\tau_{\min}\ln\left(\frac{\tau_{\max}}{\tau_{\min}}\right)} & \text{for } \alpha = 1, \\ \frac{1-\alpha}{\alpha\tau_{\max}}\left(\frac{\tau_{\max}}{\tau_{\min}}\right)^\alpha & \text{for } 0 < \alpha < 1, \\ \frac{1}{\theta_c} & \text{for } \alpha > 1. \end{cases} \tag{36}$$

In the above we have simplified the approximation by using the assumption that pulse duration is comparatively long, $\theta_c \gg \tau_{\min}$. We are focusing on this particular case because pure $1/f$ noise will be observed only if this assumption holds. As can be seen from Eq. (36), in $T \gg \tau_{\max}$ case $\bar{\nu}$ will take a constant value dependent only on the physical parameters of the process. As shown in the earlier sections in the ergodic case, pure $1/f$ noise can be observed over an arbitrarily broad range of frequencies, which is limited by the selection of θ_c, $\tau_{\min}$ and $\tau_{\max}$. In the low frequency range power spectral density of the process devolves into white noise, and in the high frequency range power spectral density of the process will become Brownian-like. Thus, in the ergodic case the power spectral density is trivially integrable independently of the selected pulse and gap duration distributions or their parameters.

We can partially eliminate low-frequency cutoff by sampling gap durations from the Pareto distribution without an upper bound, but in this case we need to consider finiteness of the observation time T and the integrability paradox. Note that the low-frequency cutoff may still be observed if $\frac{1}{T} \lesssim f^{(c)}$, but otherwise pure $1/f$ noise will be observed starting from the smallest observable frequency (see Fig. 5 for the simulated power spectral density).

If $T \leqslant \tau_{\max}$ then the observed distribution of gap durations is effectively bounded by T, and thus the mean number of pulses would be given by Eq. (36), but with $\tau_{\max}$ replaced by T. Notably, for $\alpha \leqslant 1$ mean number of pulses depends on the observation time

$$\bar{\nu} \propto \begin{cases} \frac{1}{\ln(T)} & \text{for } \alpha = 1, \\ T^{\alpha-1} & \text{for } 0 < \alpha < 1, \\ \text{const} & \text{for } \alpha > 1. \end{cases} \quad (37)$$

Note that $T \leqslant \tau_{\max}$ assumption doesn't affect the derivations presented in the earlier sections, or their implications. Results similar to those shown in Fig. 5 could be also obtained with the ergodic model, but with an obvious low-frequency cutoff. Equation (31) and, more generally, Eq. (33) apply to the weakly nonergodic case as well as they do for the ergodic case. Introduction of finite observation time T only changes the fact that for the most parameter sets the low-frequency cutoff will be unobservable. It also introduces aging effects into the power spectral densities. Integrating the power spectral density for the comparatively long pulse duration case $\theta_c \gg \tau_{\min}$, combining the approximations Eq. (27) and Eq. (16), yields

$$\int_{1/T}^{\infty} S(f) df \approx 4a^2\bar{\nu} \times \frac{\tau_{\min}^{\alpha}\Gamma(1-\alpha)\cos\left(\frac{\pi\alpha}{2}\right)}{(2\pi)^{2-\alpha}} \times \int_{1/T}^{\frac{1}{2\pi\tau_{\min}}} \frac{df}{f^{2-\alpha}} + \frac{a^2\bar{\nu}}{\pi^2}\int_{\frac{1}{2\pi\tau_{\min}}}^{\infty}\frac{df}{f^2}$$

$$= \frac{2}{\pi}a^2\bar{\nu}\tau_{\min} + \begin{cases} a^2\bar{\nu}\tau_{\min} \times \ln\left(\frac{T}{2\pi\tau_{\min}}\right) & \text{for } \alpha = 1, \\ a^2\bar{\nu}\tau_{\min}^{\alpha} \times \frac{4\Gamma(1-\alpha)\cos\left(\frac{\pi\alpha}{2}\right)}{(2\pi)^{2-\alpha}} \times \frac{T^{1-\alpha}-(2\pi\tau_{\min})^{1-\alpha}}{1-\alpha} & \text{otherwise.} \end{cases} \quad (38)$$

Inserting Eq. (37) into Eq. (38) we can see that the power spectral density is integrable and finite, but depends on the observation time

$$\int_{1/T}^{\infty} S(f) df \propto \begin{cases} \frac{1}{\ln(T)} & \text{for } \alpha = 1, \\ \frac{1}{T^{1-\alpha}} & \text{for } 0 < \alpha < 1, \\ \frac{1}{T^{\alpha-1}} & \text{for } \alpha > 1. \end{cases} \quad (39)$$

Similar observations of aging effects in the power spectral densities of signals with rectangular pulses were made in the experiments involving blinking quantum dots and their theoretical modeling treatments [50–52]. Aging effects are not as clearly visible in Fig. 5, because we have focused on the case reproducing $1/f$ noise, while in this case the dependence on the observation time is logarithmically slow. For the other choices of α, the dependence would be much more obvious.

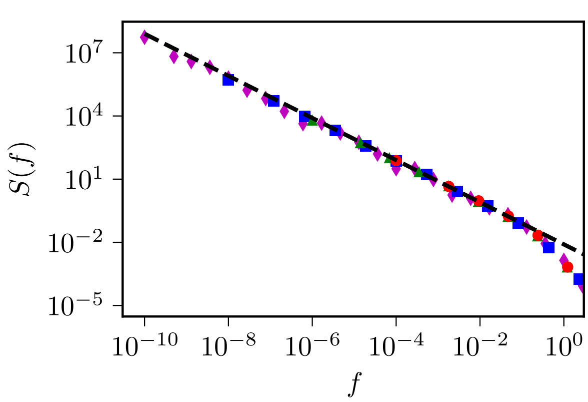

FIG. 5. Comparison of the power spectral densities in the weakly nonergodic case. Different curves correspond to different observations times: $T = 10^4$ (red circles), 10^6 (green triangles), 10^8 (blue squares), and 10^{10} (magenta diamonds). Gap durations were sampled from the Pareto distribution (with $\alpha = 1$ and $\tau_{\min} = 1$), unit size ($a = 1$) pulse durations were sampled from the exponential distribution (with $\theta_c = 10^2$). Dashed black line has $1/f$ slope.

VI. CONCLUSIONS

We have investigated the power spectral density of a signal consisting from nonoverlapping rectangular pulses. We have also considered point process limit of the process and found that point processes can not yield pure $1/f$ noise. To obtain pure $1/f$ noise one needs to have power-law distributed gap (or pulse) durations, while the characteristic pulse (or gap) duration needs to be long in comparison to characteristic gap (or pulse) duration. If the characteristic pulse (or gap) duration is short, extreme case corresponding to a point process, then $1/f$ dependence will be perverted by an additional term logarithmically dependent on f. In our analysis we have assumed that gap durations are sampled from the bounded Pareto distribution, while pulse durations may be sampled from various distributions with short or long characteristic durations. Due to the symmetry of the general expression for the power spectral density [Eq. (12)] in respect to the characteristic functions of pulse and gap duration distributions, our analysis and conclusions remain valid even if the assumptions about gap and pulse duration distributions would be swapped. Our result to certain extent supplements and contrasts earlier investigations into the power-law distributed pulse (or gap) durations (such as Refs. [13,39,40]).

As the approximation of the power spectral density [Eq. (31)] doesn't explicitly depend on the maximum bound of the gap duration distribution $\tau_{\max}$, gap durations could also be sampled from the Pareto distribution without a maximum bound. This leads to a weakly nonergodic case of the process similar to the one considered in Ref. [13]. In contrast to Ref. [13] we predict that cutoff may be found, but at extremely low frequency $f^{(c)}$. It arises due to logarithmic term present in Eq. (28), and consequently in Eq. (29), becoming non-negligible at frequencies lower than

$f^{(c)}$. Though due to implicit dependence of $\bar{\nu}$ on the $\tau_{\max}$, when $T \leqslant \tau_{\max}$ aging effects will be observed as discussed in Refs. [50–52].

Future extensions of the approach presented here could include consideration of general pulse shapes, overlaps between the pulses, and multiple trap or particle dynamics (a signal is then constructed from multiple telegraphlike signals or single-particle systems).

All of the code used to perform the reported numerical simulations is available in Ref. [66].

Author contributions from A.K. include software, validation, original draft writing, review, and editing, and visualization. Author contributions from B.K. include conceptualization, methodology, original draft writing, review, and editing.

[1] J. B. Johnson, Phys. Rev. **26**, 71 (1925).
[2] W. Schottky, Phys. Rev. **28**, 74 (1926).
[3] R. F. Voss and J. Clarke, Nature (London) **258**, 317 (1975).
[4] W. H. Press, Flicker noises in astronomy and elsewhere, Comments on Modern Physics, Part C-Comments on Astrophysics **7**, 103 (1978).
[5] P. Dutta and P. M. Horn, Rev. Mod. Phys. **53**, 497 (1981).
[6] M. Kobayashi and T. Musha, IEEE Trans. Biomed. Eng. **29**, 456 (1982).
[7] R. Cont, Quant. Financ. **1**, 223 (2001).
[8] F. N. Hooge, T. G. M. Kleinpenning, and L. K. J. Vandamme, Rep. Prog. Phys. **44**, 479 (1981).
[9] S. Kogan, *Electronic Noise and Fluctuations in Solids* (Cambridge University Press, 1996).
[10] H. Wong, Microelectronics Reliability **43**, 585 (2003).
[11] B. B. Mandelbrot and J. R. Wallis, Water Resour. Res. **5**, 321 (1969).
[12] M. A. Caloyannides, J. Appl. Phys. **45**, 307 (1974).
[13] M. Niemann, H. Kantz, and E. Barkai, Phys. Rev. Lett. **110**, 140603 (2013).
[14] K. L. Schick and A. A. Verveen, Nature (London) **251**, 599 (1974).
[15] G. Careri and G. Consolini, Phys. Rev. E **62**, 4454 (2000).
[16] Z. Siwy and A. Fuliński, Phys. Rev. Lett. **89**, 158101 (2002).
[17] J. Beran, *Statistics for Long-Memory Processes*, 1st ed. (Routledge, New York, 2017), p. 315.
[18] T. Bollerslev, Glossary to ARCH (GARCH), CREATES Research Paper (2008).
[19] K. Burnecki and A. Weron, J. Stat. Mech. (2014) P10036.
[20] A. L. McWhorter and R. H. Kingston, in *Proceedings of the Conference on Physics of Semiconductor Surface Physics*, Vol. 207 (University of Pennsylvania, Philadelphia, 1957).
[21] B. Kaulakys, V. Gontis, and M. Alaburda, Phys. Rev. E **71**, 051105 (2005).
[22] P. Bak, C. Tang, and K. Wiesenfeld, Phys. Rev. Lett. **59**, 381 (1987).
[23] A. C. Yadav, R. Ramaswamy, and D. Dhar, Europhys. Lett. **103**, 60004 (2013).
[24] B. Kaulakys and T. Meskauskas, Phys. Rev. E **58**, 7013 (1998).
[25] B. Kaulakys and M. Alaburda, J. Stat. Mech. (2009) P02051.
[26] J. Ruseckas, R. Kazakevicius, and B. Kaulakys, J. Stat. Mech. (2016), 043209.
[27] A. Kononovicius and V. Gontis, Physica A **391**, 1309 (2012).
[28] R. Kazakevicius, A. Kononovicius, B. Kaulakys, and V. Gontis, Entropy **23**, 1125 (2021).
[29] J. L. McCauley, G. H. Gunaratne, and K. E. Bassler, Physica A **379**, 1 (2007).
[30] I. Eliazar, J. Phys. A: Math. Theor. **54**, 35LT01 (2021).
[31] A. C. Yadav and N. Kumar (2021), arXiv:2103.11608 [cond-mat.stat-mech].
[32] R. Kazakevicius and A. Kononovicius, Phys. Rev. E **103**, 032154 (2021).
[33] F. Mainardi, R. Gorenflo, and A. Vivoli, J. Comput. Appl. Math. **205**, 725 (2007).
[34] T. Lukes, Proc. Phys. Soc. **78**, 153 (1961).
[35] D. Halford, Proc. IEEE **56**, 251 (1968).
[36] C. Heiden, Phys. Rev. **188**, 319 (1969).
[37] T. H. Bell, J. Appl. Phys. **45**, 1902 (1974).
[38] J. Ruseckas, B. Kaulakys, and M. Alaburda, Lith. J. Phys. **43**, 223 (2003).
[39] G. Margolin and E. Barkai, J. Stat. Phys. **122**, 137 (2006).
[40] M. Lukovic and P. Grigolini, J. Chem. Phys. **129**, 184102 (2008).
[41] L. Cywinski, R. M. Lutchyn, C. P. Nave, and S. Das Sarma, Phys. Rev. B **77**, 174509 (2008).
[42] J.-O. Krisponeit, C. Kalkert, B. Damaschke, V. Moshnyaga, and K. Samwer, Phys. Rev. B **87**, 121103(R) (2013).
[43] I. Eliazar, Phys. Rev. E **87**, 052125 (2013).
[44] G. Wirth, Solid-State Electron. **186**, 108140 (2021).
[45] G. Wirth, M. B. da Silva, and T. H. Both, in *2021 5th IEEE Electron Devices Technology and Manufacturing Conference (EDTM)* (IEEE, 2021).
[46] A. Rehman, J. A. D. Notario, J. S. Sanchez, Y. M. Meziani, G. Cywiński, W. Knap, A. A. Balandin, M. Levinshtein, and S. Rumyantsev, Nanoscale **14**, 7242 (2022).
[47] J. Pyo, A. Ihara, and S. ichiro Ohmi, Jpn. J. Appl. Phys. **61**, SC1066 (2022).
[48] F. Gruneis, Phys. Lett. A **383**, 1401 (2019).
[49] F. Gruneis, Phys. Lett. A **384**, 126145 (2020).
[50] S. Sadegh, E. Barkai, and D. Krapf, New J. Phys. **16**, 113054 (2014).
[51] N. Leibovich, A. Dechant, E. Lutz, and E. Barkai, Phys. Rev. E **94**, 052130 (2016).
[52] N. Leibovich and E. Barkai, Phys. Rev. E **96**, 032132 (2017).
[53] R. N. Munoz, L. Frazer, G. Yuan, P. Mulvaney, F. A. Pollock, and K. Modi, Phys. Rev. E **106**, 014127 (2022).
[54] Y. M. Blanter and M. Buttiker, Phys. Rep. **336**, 1 (2000).
[55] V. Mitin, L. Reggiani, and L. Varani, Generation-recombination noise in semiconductors, in *Noise and Fluctuation Controls in Electronic Devices*, Noise and Fluctuation Controls in Electronic Devices (American Scientific Publishers, 2002).
[56] D. F. Anderson and T. G. Kurtz, in *Design and Analysis of Biomolecular Circuits* (Springer New York, 2011) pp. 3–42.
[57] M. Levene and A. Kononovicius, Commun. Stat. Simul. Comput. **50**, 3751 (2019).
[58] G. Fibich, Phys. Rev. E **94**, 032305 (2016).

[59] A. Clauset, C. Shalizi, and M. Newman, SIAM Rev. **51**, 661 (2009).

[60] A. Stanislavsky, K. Weron, and A. Weron, Commun. Nonlinear Sci. Numer. Simul. **24**, 117 (2015).

[61] S. Begusic, Z. Kostanjcar, H. E. Stanley, and B. Podobnik, Physica A **510**, 400 (2018).

[62] M. Karsai, Computational human dynamics, arXiv:1907.07475.

[63] P. Frantsuzov, M. Kuno, B. Jankó, and R. A. Marcus, Nat. Phys. **4**, 519 (2008).

[64] Z. R. Fox, E. Barkai, and D. Krapf, Nat. Commun. **12**, 6162 (2021).

[65] O. Vilk, E. Aghion, R. Nathan, S. Toledo, R. Metzler, and M. Assaf, J. Phys. A **55**, 334004 (2022).

[66] https://github.com/akononovicius/flicker-snorp.